Revista de Chimie
https://revistadechimie.ro
https://doi.org/10.37358/Rev. Chim.1949

Hydrolysis Mechanism of Bismuth in Chlorine Salt System Calculated by Density Functional Method

LIAO CHUNFA , XU ZHENXIN, ZOU JIANBAI , JIANG PINGGUO*#
Faculty of Materials, Metallurgy and Chemistry, Jiangxi University of Science and Technology, Ganzhou 341000, China

Abstract: *Based on the density functional theory, this paper presents the calculated cellular electronic properties of $BiCl_3$, BiOCl and Bi_3O_4Cl, including unit cell energy, band structure, total density of states, partial density of states, Mulliken population, overlapping population, etc. Combined with the thermodynamic analysis of Bi^{3+} hydrolysis process in chlorine salt system, the conversion mechanism of oxychloride bond in $BiCl_3$ to form BiOCl and Bi_3O_4Cl by hydrolysis, ethanololysis and ethylene glycol alcohololysis was obtained by infrared spectroscopy. The results indicate that the energy of Bi_3O_4Cl cell system was lower than that of BiOCl cell, indicating that the structure of Bi_3O_4Cl was more stable. From the analysis of bond fluctuation, the electron nonlocality in BiOCl belt was relatively large, and the orbital expansibility was strong; thus the structure of BiOCl was relatively active. The state density map of Bi_3O_4Cl had the widest energy gap, i.e., the covalent bond between Bi_3O_4Cl was stronger than BiOCl. Therefore, the hydrolysis of $BiCl_3$ would preferentially generate Bi_3O_4Cl with a more stable structure. The number of charge arrangement, overlapping population and infrared spectrogram indicate that there were two basic ways in the hydrolysis and alcoholysis of $BiCl_3$. Firstly, two chlorine atoms in $BiCl_3$ were replaced by hydroxyl groups ionized by water and alcohol to form $[Bi(OH)_2Cl]$ monomer, and BiOCl and Bi_3O_4Cl were formed by intra-molecular dehydration or inter-molecular dehydration. The other way was that the Bi atom directly reacted with the OH ionized by water and alcohol to form the [Bi-OH] monomer, and the Cl atom replaced the H atom on the hydroxyl group in the [Bi-OH] monomer to further form BiOCl and Bi_3O_4Cl.*

Keywords: *Density functional method, Bi^{3+} hydrolysis mechanism, unit cell structure, infrared spectrum*

1.Introduction

Bismuth is mainly present in bismuthinite (Bi_2S_3), bismuth ochre (Bi_2O_3), bismuthinite ($nBi_2O_3 \cdot mCO_2 \cdot H_2O$), bismuth copper ore ($3Cu_2S_4 \cdot Bi_2S_3$) and other minerals. In many heavy metal smelting processes, a small amount of bismuth is often concentrated in the by-products, such as copper anode slime, lead anode slime, copper smelting and converting dusts, etc. [1-4]. Arsenic, antimony and bismuth in the anode slime of copper and lead are wrapped with embedded adhesion, which leads to the difficulty of efficiently leaching and deep separation of rare precious metals. After complex acid leaching, arsenic, antimony and bismuth enter into the acid leaching solution. Antimony and bismuth will be hydrolyzed into chlorine oxide precipitation by adjusting the *p*H of the acid leaching solution, and then they are separated. Therefore, clarification of the behaviors of antimony and bismuth in solution and the hydrolysis separation mechanism is the key to realize an efficient and collaborative leaching process of the associated metals in anode slime.

Bismuth is widely used in metallurgy, medicine, chemical industry, photo catalyst, semiconductor, superconductor, nuclear industry material, environmental pollution treatment, etc. [5-11] Among them, lanthanidephoto catalysts are generally divided into lanthanide-based photocatalysts and lanthanide composite photocatalysts. Methods to prepare them generally include hydrolysis method [12-13], glycol-solvent-thermal method [14-15], extraction method [16] and so on. Currently, the researches on mechanism of bismuth oxide preparation by bismuth powder [17-20] and dechlorination of bismuth

*email: pingguo jiang@163.com #Fund Project: Project supported by the National Natural Science Foundation of China (U1802251) Funded by the National Natural Science Foundation of China (51564016) Funded by Jiangxi Provincial Department of Education Science and Technology Project (GJJ180466)

oxychloride to form the bismuth oxide [21-22] have been extensively reported. However, the mechanism of bismuth oxide hydrolysis preparation by bismuth chloride compound photo catalyst has not been reported. The present study was thus motivated.

To explore the element hydrolysis mechanisms for the preparation of bismuth oxychloride, in this paper, electronic structure of $BiCl_3$, BiOCl, Bi_3O_4Cl was calculated using density functional method. The formation mechanisms was explored from the respects of cell structure, band structure, density of states, charge layout number and overlapping inhabit in $BiCl_3$ basic reaction and process of hydrolysis, alcohol solution, and further confirmed by infrared spectrum from the perspective of valence change.

2. Materials an methods

2.1 Structure design and calculation of bismuth compounds

Based on the first principle density functional theory (DFT), combined with the CASTEP[23-24] module of the planar pseudopotential method, the cell structure of bismuth compounds was optimized, and the energy band structure, total state density and separation density, charge arrangement number and overlap polymerization number were calculated. $BiCl_3$, BiOCl and Bi_3O_4Cl cell models were established according to relevant parameters shown in Table 1. The exchange effect of electron - electron interaction between crystal cells was corrected by general gradient approximation (GGA). PBE in GGA was adopted to deal with the interaction correlation energy between electrons. The grid points of k-space were selected by the Monkhorst-Pack scheme, and the total energy and charge density of the system were integrated in the Brillouin zone. The k-vectors of the Brillouin zone was selected as 1×2×2, 5×5×2, and 5 × 5 × 4; plane wave truncation could be set to 258.5 eV, 489.8 eV and 489.8 eV, respectively. The self-consistent precision was set to be 2.0×10^{-6} eV / atom, and the force acting on each atom did not not exceed 0.05 eV /nm.

Table 1. Unit cell parameters

Title	Space group name	Lattice parameters					
		a	b	c	α	β	γ
$BiCl_3$	P n 21 a	7.64100Å	9.17200Å	6.29100Å	90.0000°	90.0000°	90.0000°
BiOCl	P 4/n m m	3.88300Å	3.88300Å	7.34700Å	90.0000°	90.0000°	90.0000°
Bi_3O_4Cl	I 2/a	5.69540Å	5.64760Å	18.57300Å	90.0000°	91.5230°	90.0000°

2.2. Infrared spectrum analysis — Bi^{3+} hydrolysis experiment in chlorine salt system

$BiCl_3$ in two solid and liquid states was hydrolyzed and alcoholylyzed in different systems. $BiCl_3$ solid powder and its solution (0.17 mol/LBi^{3+}, 1 mol/L Cl^-) were mixed with the same amount of deionized water, ethanol and ethylene glycol at 25℃ (water bath) for 2 h. Then the solutions were adjusted to *p*H=4 and treated in the ultrasonic cleaner ultrasonic for 1 hour. The precipitation was achieved by centrifugal method and filtrated with repeated washing, and the product was obtained after drying at 60℃ for 6 h. All the experiments were performed by blank experiment, i.e., to determine the infrared spectrum of the same volume of deionized water, ethanol, ethylene glycol and hydrochloric acid.

3 Results and discussions

3.1 First principle analysis of bismuth compounds

3.1.1 Energy analysis of bismuth compounds

The until cell structure of $BiCl_3$, BiOCl and Bi_3O_4Cl from structure optimization and energy calculation are shown in Table 2. It has been reported that the lower the total cell energy, the more stable the cell structure [25-27]. The cell energy of Bi_3O_4Cl was lower than that of BiOCl. Therefore, Bi_3O_4Cl was preferential to form stable structure when $BiCl_3$ was hydrolyzed.

Table 2. Total cell energy

Material	Energy
$BiCl_3$	-13586.9255 eV
BiOCl	-5980.5754 eV
Bi_3O_4Cl	-17125.1236 eV

3.1.2 Band analysis of bismuth compounds

As shown in Figure 1, $BiCl_3$ had a band width of 37.2 eV and a forbidden band width of 3.996 eV; BiOCl had a band width of 38.8 eV and a forbidden band width of 2.707 eV; while Bi_3O_4Cl had a band width of 40.5 eV and a forbidden band width of 2.704 eV.

The wider the width of the energy band was, the larger the undulation was, the smaller the effective mass of the electrons in the energy band was, and the larger the degree of non-locality was, the stronger the atomic orbital scalability of the energy band was ,and the more active nature was. On the contrary, the narrower band indicates that the eigenstate corresponding to this band was mainly composed of atomic orbitals of a certain grid point in the local area. The electron locality of this band was very strong, the orbital expansion was weak, and the nature was stable [28-29].

Therefore, it can be seen from Figure 1 that the energy bandwidth of BiOCl was smaller than the bandwidth of Bi_3O_4Cl, and the undulation of the BiOCl band was relatively larger than that of Bi_3O_4Cl. Therefore, in terms of band width, BiOCl was narrower, the electron locality of the band was stronger, the orbital expansion was weak, and the property was relatively stable. From the band undulation, Bi_3O_4Cl had a small degree of undulation and could carry electrons. The degree of non-locality was small, the orbital expansion was weak, and the nature was relatively stable. The stabilities of BiOCl and Bi_3O_4Cl would be further analyzed.

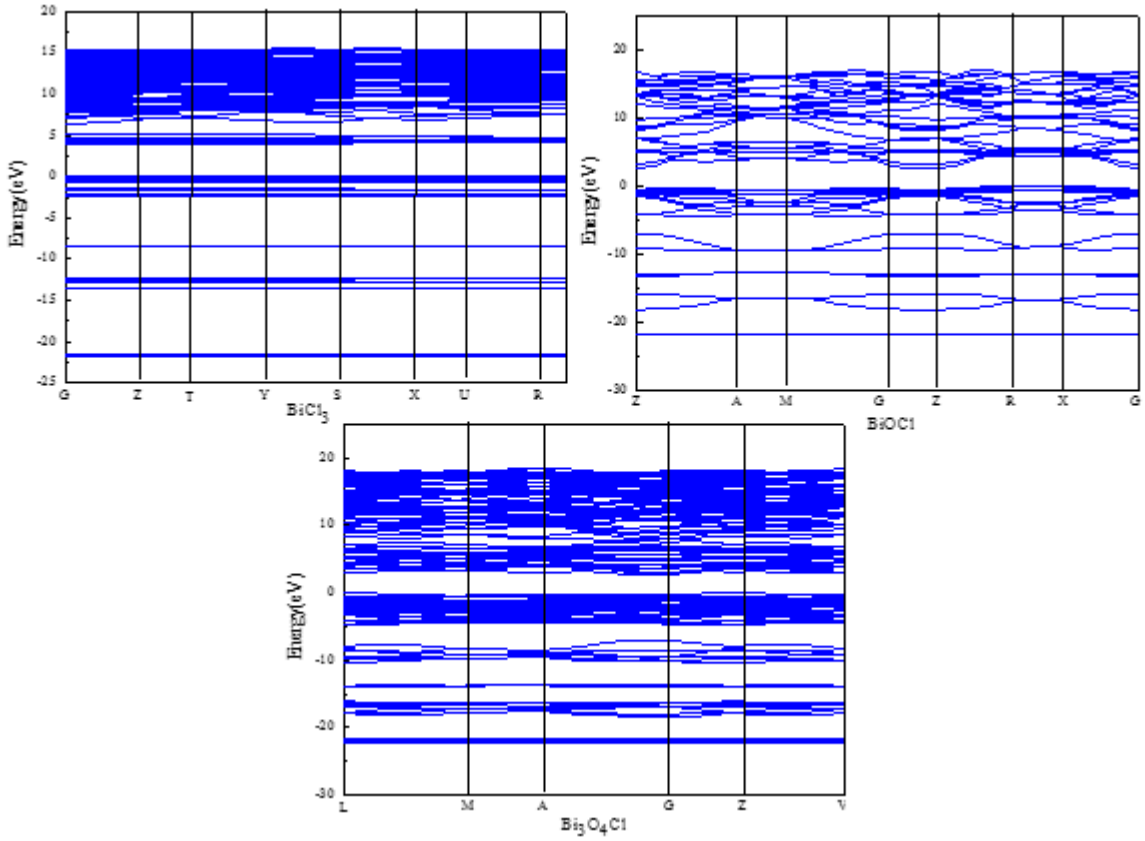

Figure 1. $BiCl_3$, BiOCl, Bi_3O_4Cl energy band diagram

3.1.3 Analysis of bismuth compounds about density of state

Figure 2 shows that the valence band (-21.9-0 eV) of $BiCl_3$ was mainly formed by the electron states of Bi 6s6p and Cl 2s2p; the conduction band (0-15.3 eV) was excited by the electron states of Cl 2p and Bi 6p, and the peak value at the Fermi energy level was mainly associated to the electron orbitals of Cl 2p and Bi 6p.

Regarding the BiOCl, the valence band (-21.9-0 eV) was mainly formed by the electronic states of Bi 6s6p5d, O 2s2p and Cl 2s2p, while the conductance band (0—16.9 eV) was assigned to the electronic states of Bi 6s6p5d, O 2s2p and Cl 2s2p.

Regarding the Bi_3O_4Cl, the valence band (-22.4-0 eV) was mainly formed by the electron states of Bi 6s6p, O 2s2p and Cl 2s2p, and the conduction band (0-18.1 eV) was assigned to the electron states of O 2p and Bi 6s6p. The peak value at the Fermi level was mainly contributed by the electron orbitals of Cl 2p, O 2p and Bi 6s6p.

Because the size of the pseudo gap (the peak and valley of the low-energy bonding state and the high-energy anti-bonding state are defined as the pseudo gap) of the state density map can reflect the strength of covalent bonds. The wider the pseudoenergy gap is, the stronger the covalency is. The larger the horizontal coordinate of the peak state density is, the easier it is for the electrons outside the nucleus to be distributed in the high energy region, and the easier it is to lose electrons; otherwise, the easier it is to gain electrons [30-31].

Therefore, according to the state density diagram in Figure 2, $BiCl_3$ had a pseudoenergy gap of -0.2285-4.3836 eV, and a pseudoenergy gap width of 4.6121 eV, which was mainly excited by the electrons in the electron orbitals of Cl 2p and Bi 6p. BiOCl had a pseudoenergy gap of -0.7358-4.6202 eV, and a pseudoenergy gap of 5.356 eV, mainly assigned to the electrons in the electron orbitals of Cl 2p, O 2p and Bi 6s6p. Bi_3O_4Cl had a pseudoenergy gap of -1.6698-5.0294 eV and a pseudoenergy gap of 6.6992 eV, mainly associated to electrons in the electron orbitals of Cl 2p, O 2p and Bi 6s6p. Comparing the pseudoenergy gap width of $BiCl_3$, BiOCl and Bi_3O_4Cl, *viz.* $BiCl_3$<BiOCl<Bi_3O_4Cl, the covalent bond between Bi_3O_4Cl atoms was stronger than $BiCl_3$ and BiOCl. This suggested that $BiCl_3$ hydrolysis was more likely to produce relatively stable Bi_3O_4Cl.

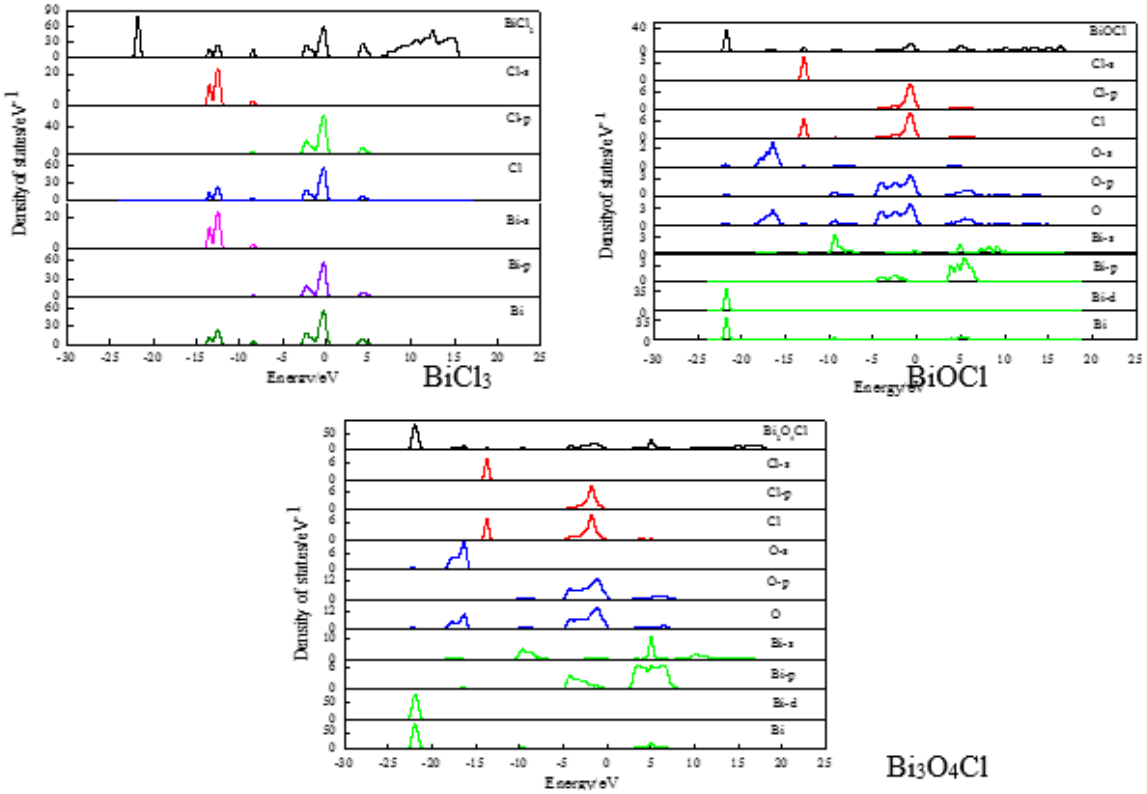

Figure 2. Density and density of states of $BiCl_3$, BiOCl and Bi_3O_4Cl

3.1.4 Analysis of the charge layout of bismuth compounds

The number of charge layouts can reflect the gain and loss of atomic electrons. A positive charge indicates the loss of electrons, and a negative charge indicates the gain of electrons. The gain and loss of electrons can feedback the strength of the bond interaction between atoms. The more electrons are transferred, the stronger the bond interaction between atoms will be, and vice versa [32].

Table 3 shows that each $BiCl_3$ crystal cell contained 12 Cl atoms, among which 8 Cl atoms got 0.42 electrons and 4 Cl atoms got 0.45 electrons respectively. Four Bi atoms, each of them lost 1.29 electrons. Each Bi atom lot an electron from two Cl atoms that gained an electron of 0.42 and one Cl atom that gained an electron of 0.45. The more electrons are transferred, the stronger the interaction between atomic bonds will be. Therefore, in $BiCl_3$ structure, the interaction between the two groups of [Bi-Cl] bonds was weaker than that of the other group. Therefore, $BiCl_3$ preferentially would break up two groups of [Bi-Cl] bonds with weak interaction during hydrolysis to form $Bi(OH)_2Cl$.

BiOCl cell contained 2 groups [BiOCl], in which each Bi atom lost 1.48 electrons, each Cl atom gained 0.56 electrons, and each O atom gained 0.92 electrons. The electrons lost by each Bi atom were gained by one Cl atom and one O atom. The more electrons are transferred, the stronger the bond interaction between atoms will be; thus, the bond interaction between [Bi-O] was stronger than that between [Bi-Cl], which was easy to remove Cl ions in the later stage, and to refine Bi_2O_3 or Bi powder.

According to the charge layout number of Bi_3O_4Cl, 8 O atoms got 0.96 electrons and 4 O atoms got 0.97 electrons. Two Cl atoms gained 0.62 electrons. Four of the six Bi atoms lost 1.45 electrons, and two of them lost 1.58 electrons. The Bi atom losing 1.45 electrons existed in the form of [BiO_2-O-BiO_2], and the two Bi atoms lose a total of 2.9 electrons, which was obtained by two 0.97 O atoms and one 0.96 O atoms. The Bi-O bond interaction between [BiO_2-O-BiO_2] (or [Bi_2O_3]) was stronger than the Bi-O bond interaction between the O atoms shared by [BiO_2-O-BiO_2]. The Bi atom losing 1.58 electrons was obtained by a 0.62 Cl atom and a 0.96 O atom in the form of [BiOCl], wherein the Bi-O bond was stronger than the Bi-Cl bond.

Table 3. Charge layout number

Unitcell	Species	Ion	s	p	d	f	Total	Charge(e)
$BiCl_3$	Cl	1	1.97	5.45	0.00	0.00	7.42	-0.42
	Cl	2	1.97	5.45	0.00	0.00	7.42	-0.42
	Cl	3	1.98	5.47	0.00	0.00	7.45	-0.45
	Cl	4	1.97	5.45	0.00	0.00	7.42	-0.42
	Cl	5	1.97	5.45	0.00	0.00	7.42	-0.42
	Cl	6	1.98	5.47	0.00	0.00	7.45	-0.45
	Cl	7	1.97	5.45	0.00	0.00	7.42	-0.42
	Cl	8	1.97	5.45	0.00	0.00	7.42	-0.42
	Cl	9	1.98	5.47	0.00	0.00	7.45	-0.45
	Cl	10	1.97	5.45	0.00	0.00	7.42	-0.42
	Cl	11	1.97	5.45	0.00	0.00	7.42	-0.42
	Cl	12	1.98	5.47	0.00	0.00	7.45	-0.45
	Bi	1	1.96	1.75	10.00	0.00	13.71	1.29
	Bi	2	1.96	1.75	10.00	0.00	13.71	1.29
	Bi	3	1.96	1.75	10.00	0.00	13.71	1.29
	Bi	4	1.96	1.75	10.00	0.00	13.71	1.29
BiOCl	O	1	1.92	5.00	0.00	0.00	6.92	-0.92
	O	2	1.92	5.00	0.00	0.00	6.92	-0.92
	Cl	1	1.97	5.59	0.00	0.00	7.56	-0.56
	Cl	2	1.97	5.59	0.00	0.00	7.56	-0.56
	Bi	1	1.95	1.57	0.00	10.00	13.52	1.48
	Bi	2	1.95	1.57	0.00	10.00	13.52	1.48
Bi_3O_4Cl	O	1	1.92	5.04	0.00	0.00	6.96	-0.96
	O	2	1.91	5.06	0.00	0.00	6.97	-0.97
	O	3	1.92	5.04	0.00	0.00	6.96	-0.96
	O	4	1.91	5.06	0.00	0.00	6.97	-0.97
	O	5	1.92	5.04	0.00	0.00	6.96	-0.96
	O	6	1.91	5.06	0.00	0.00	6.97	-0.97

O	7	1.92	5.04	0.00	0.00	6.96	-0.96
O	8	1.91	5.06	0.00	0.00	6.97	-0.97
Cl	1	1.97	5.65	0.00	0.00	7.62	-0.62
Cl	2	1.97	5.65	0.00	0.00	7.62	-0.62
Bi	1	1.88	1.68	10.00	0.00	13.55	1.45
Bi	2	1.88	1.68	10.00	0.00	13.55	1.45
Bi	3	1.88	1.68	10.00	0.00	13.55	1.45
Bi	4	1.88	1.68	10.00	0.00	13.55	1.45
Bi	5	1.94	1.48	10.00	0.00	13.42	1.58
Bi	6	1.94	1.48	10.00	0.00	13.42	1.58

3.1.5 Analysis of overlapping concentration number of bismuth compounds

The overlapping population can be used to express the interaction between atoms, analyze the bonding properties between atoms, and identify the bonding strength between atoms. When the number of overlapping population is positive, the bonding between atoms is covalent bond. The larger the value is, the stronger the covalent bond is and the more stable the structure is. When the overlapping population is negative, the bonding between atoms is antibonding. The smaller the value is, the stronger the repulsion between atoms is, and the worse the stability of crystal cells is. When the overlap concentration number is 0, there are ionic bonds between atoms [33-35]. The overlapping population of $BiCl_3$, BiOCl and Bi_3O_4Cl are shown in Table 4.

The positive overlapping population of $BiCl_3$ indicates that the chemical bond between the Cl atom and the Bi atom was covalently bonded. The population of the four groups of Bi-Cl bonds was 0.30, and the population of the eight groups of Bi-Cl bonds was 0.28. The larger the population, the stronger the stability of the covalent bond. Each [$BiCl_3$] unit contained a Bi-Cl bond with a population of 0.30 and two Bi-Cl bonds with a population of 0.28; thus, hydrolysis occurred when $BiCl_3$ was dissolved in water, followed by that the hydroxide generated by water ionization was replaced. Two of the Cl atoms in the Bi-Cl bond with a population of 0.28 formed $Bi(OH)_2Cl$, which further formed BiOCl, which was consistent with the above-mentioned charge distribution number analysis.

The positive overlapping population of BiOCl meant that the chemical bonds between O and Bi atoms were covalently bonded, i.e., the total overlap population was 1.12. The overlapping population of O-O was -0.23 (<0), which meant that the O-O bond formed an anti-bond, i.e., the two O atoms were mutually exclusive. The smaller the negative value, the stronger the inter-atomic repulsive force. The stability of the unit cell was therefore lower.

It is known from the overlap of Bi_3O_4Cl that the O-Bi bond can form a covalent bond or an anti-bond. The 24 groups of O-Bi bonds were covalently linked, and the total overlap population were 4.2. The anti-bonds were formed between the 4 groups of O-Bi bonds, and the total overlap population was -0.04. The negative overlap of 10 groups of O-O bonds was less than 0, indicating that the 10 groups of O-O bonds were formed with anti-bonds, i.e., the total overlap population was -0.66. The smaller the overlapping population of the anti-bonds, the atoms representing the anti-bonds were received in the unit cell would suffer greater the repulsive force, the more unstable the unit cell.

Comparing the size and number of overlapping populations of BiOCl and Bi_3O_4Cl, we can see that the total number of overlapping populations of BiOCl covalent bonds was 1.12, the total number of overlapping populations of anti-bonds was -0.28, the total number of overlapping populations of covalent bonds, and the overlap of anti-bond. The sum of the total number of settlements was 0.84, and the effect of covalent bonds was 4 times that of reverse bonds [36-37]. The greater the role of covalent bonds, the more stable the structure; the total number of overlapping settlements of Bi_3O_4Cl covalent bonds was 4.20. The sum of the numbers was -0.70, the sum of the number of overlapping settlements of covalent bonds, the number of overlapping settlements of anti-bonds was 3.50, and thus, the effect of covalent bonds was 6 times that of reverse bonds. It can be seen that Bi_3O_4Cl had a stronger covalent bond between atoms than BiOCl, and the interaction force between atoms was large, i.e., the stability of the unit cell Bi_3O_4Cl was higher BiOCl, and a series of Bi $(OH)_2Cl$ would be generated during the hydrolysis of $BiCl_3$. It was easier to continue to remove water to generate Bi_3O_4Cl.

Table 4. Infrared characteristic peak

Unitcell	Bond	Population	Length(A)	Unitcell	Bond	Population	Length(A)
$BiCl_3$	Cl8--Bi3	0.28	2.43173	$BiCl_3$	Cl4--Bi2	0.30	2.49005
	Cl11--Bi4	0.28	2.43173		Cl1--Bi1	0.30	2.49005
	Cl5--Bi2	0.28	2.43173		Cl9--Bi3	0.28	2.54509
	Cl2--Bi1	0.28	2.43173		Cl12--Bi4	0.28	2.54509
	Cl10--Bi4	0.30	2.49005		Cl6--Bi2	0.28	2.54509
	Cl7--Bi3	0.30	2.49005		Cl3--Bi1	0.28	2.54509
BiOCl	O2--Bi1	0.28	2.34043	BiOCl	O1--Bi2	0.28	2.34043
	O1--Bi1	0.28	2.34043		O1--O2	-0.23	2.76664
	O2--Bi2	0.28	2.34043				
Bi_3O_4Cl	O4--Bi3	0.25	2.10539	Bi_3O_4Cl	O2--Bi5	0.09	2.37242
	O2--Bi4	0.25	2.10539		O5--Bi5	0.05	2.68592
	O6--Bi2	0.25	2.10539		O1--Bi6	0.05	2.68592
	O8--Bi1	0.25	2.10539		O3--Bi6	0.05	2.68592
	O7--Bi4	0.23	2.1313		O7--Bi5	0.05	2.68592
	O5--Bi3	0.23	2.1313		O4--O8	-0.05	2.71861
	O3--Bi2	0.23	2.1313		O2--O6	-0.05	2.71861
	O1--Bi1	0.23	2.1313		O7--O8	-0.07	2.78478
	O1--Bi4	0.26	2.14494		O1--O2	-0.07	2.78478
	O5--Bi2	0.26	2.14494		O5--O6	-0.07	2.78478
	O3--Bi3	0.26	2.14494		O3--O4	-0.07	2.78478
	O7--Bi1	0.26	2.14494		O7--Bi6	-0.01	2.87273
	O8--Bi5	0.17	2.23707		O1--Bi5	-0.01	2.87273
	O4--Bi6	0.17	2.23707		O3--Bi5	-0.01	2.87273
	O2--Bi6	0.17	2.23707		O5--Bi6	-0.01	2.87273
	O6--Bi5	0.17	2.23707		O3--O5	-0.08	2.89892
	O8--Bi6	0.09	2.37242		O1--O7	-0.08	2.89892
	O4--Bi5	0.09	2.37242		O4--O6	-0.06	2.96096
	O6--Bi6	0.09	2.37242		O2--O8	-0.06	2.96096

In summary, the energy of Bi_3O_4Cl was lower than that of BiOCl, the width of constraint energy gap was: BiOCl<Bi_3O_4Cl, which suggested the covalent bond between Bi_3O_4Cl atoms was stronger than that of BiOCl, and $BiCl_3$ was more likely to form more stable Bi_3O_4Cl. The number of charge distribution shows that $BiCl_3$ was hydrolyzed. In the process, the two bonds with weak bond interaction [Bi-Cl] were preferential to be broken to form $Bi(OH)_2Cl$; the bond between [Bi-O] in BiOCl and Bi_3O_4Cl iwas stronger than [Bi-Cl], and the Cl atoms were thus easier to be removed in the later stage, and the Bi_2O_3 or Bi powder was easier to be refined. The overlapping populations of the overlapping groups / unit covalent bonds of the two unit counter bonds were further compared: Bi_3O_4Cl>BiOCl. This indicated that a series of $Bi(OH)_2Cl$ produced in the hydrolysis process of $BiCl_3$ could easily continue to remove a molecule of water to generate Bi_3O_4Cl.

In order to understand whether the fracture and formation process of valence bond during $BiCl_3$ hydrolysis was consistent with the calculated results, the thermodynamic analysis of Bi^{3+} hydrolysis process under chlorine salt system was conducted in the designed experiment, and the hydrolysis path of $BiCl_3$ and the formation mechanism of chloro-oxygen valence bond were further analyzed by infrared spectroscopy to verify the calculated results.

3.2 Thermodynamic analysis of Bi^{3+} hydrolysis process in chloride system

In the Bi^{3+}-Cl-H_2O system, Bi^{3+} was hydrolyzed at a lower *p*H, resulting in multiple solid phase intermediates including BiOCl, Bi_3O_4Cl, Bi_2O_3, and $Bi(OH)_3$. Controlling the appropriate reaction conditions could enhance Bi^{3+} to form a series of stable hydrolysates.

The stability constants of bismuth, chlorine and hydroxide ions and the standard formation molar free energy of related substances by software HSC and FactSage are listed in Table 5.

Table 5. Standard free energy of related substances at T=298K

Material	ΔfG_m^θ / (kJ·mol)	Material	ΔfG_m^θ / (kJ·mol)
H_2O	-273.178	$BiCl_3$	-155.306
OH^-	-157.293	BiOCl	-414.022
Cl^-	-131.056	Bi_3O_4Cl	-1073.233
Bi^{3+}	137.138	Bi_2O_3	-622.676
BiO^+	150.602	$Bi(OH)_3$	-740.294
BiO_2^-	-355.835		

The reaction of Bi^{3+} and Cl^- to form complex ions in Bi^{3+}-C-H_2O system is expressed by formula (1). The reaction of Bi^{3+} with OH^- forming complex ions is represented by formula (2); Bi^{3+} and Cl-formation and OH^- forming the complexing constants of the complex ions are shown in Table 6.

$$Bi^{3+}+iCl^-=BiCl_i^{3-i} \qquad \beta_i=\frac{[BiCl_i^{3-i}]}{[Bi^{3+}][Cl^-]^i} \quad (i=1\sim6) \qquad (1)$$

$$Bi^{3+}+jOH=Bi(OH)_j^{3-j} \qquad \alpha_j=\frac{[Bi(OH)_j^{3-j}]}{[Bi^{3+}][OH^-]^j} \quad (j=1\sim4) \qquad (2)$$

Table 6. The equilibrium constant of bismuth complexes

Bismuth chloride complex	$lg\beta_1$	$lg\beta_2$	$lg\beta_3$	$lg\beta_4$	$lg\beta_5$	$lg\beta_6$
Bi-Cl	2.35	4.40	5.45	6.65	7.29	7.09
Bismuth hydroxide complex	$lg\alpha_1$	$lg\alpha_2$	$lg\alpha_3$	$lg\alpha_4$	$lg\alpha_5$	$lg\alpha_6$
Bi-OH	0.0257					

The other equilibrium reactions in the Bi^{3+}—Cl—H_2O system are expressed by equations (3)-8), and the equilibrium constants are shown in Table 7.

$$Bi^{3+}+Cl^-+H_2O=BiOCl_{(s)}+2H^+ \qquad K_1=\frac{[H^+]^2}{[Bi^{3+}][Cl^-]} \qquad (3)$$

$$Bi^{3+}+H_2O=BiO^++2H^+ \qquad K_2=\frac{[H^+]^2[BiO^+]}{[Bi^{3+}]} \qquad (4)$$

$$Bi^{3+}+2H_2O=BiO_2^-+4H^+ \qquad K_3=\frac{[H^+]^4[BiO_2^-]}{[Bi^{3+}]} \qquad (5)$$

$$2Bi^{3+}+3H_2O=Bi_2O_3+6H^+ \qquad K_4=\frac{[H^+]^6}{[Bi^{3+}]^2} \qquad (6)$$

$$3Bi^{3+}+Cl^-+4H_2O=Bi_3O_4Cl_{(s)}+8H^+ \qquad K_5=\frac{[H^+]^8}{[Bi^{3+}]^3[Cl^-]} \qquad (7)$$

$$Bi^{3+}+3OH^-=Bi(OH)_{3(S)} \qquad K_{SP}=[Bi^{3+}][OH^-]^3 \qquad (8)$$

Table 7. Reaction equilibrium constant

K_1	K_2	K_3	K_4	K_5	K_{SP}
2.76×10^6	0.04	8.034×10^{-22}	1.42×10^9	8.905×10^{12}	2.99×10^{-41}

According to the simultaneous equilibrium principle, the equilibrium equation of each ion in solution could be obtained from the reactions listed above. The total concentration of Bi in the solution was denoted as $[Bi^{3+}]_T$, the free concentration of Bi ion in the solution was denoted as $[Bi^{3+}]$, the total concentration of chlorine ion in the solution was denoted as $[Cl^-]_T$, and the free concentration of Cl ion in the solution was denoted as $[Cl^-]$, then we could obtain the following equations:

$$[Bi^{3+}]_T=[Bi^{3+}]+\sum_{i=1}^{6}[BiCl_i^{3-i}]+\sum_{j=1}^{4}[Bi(OH)_j^{3-j}]+[BiO^+]+[BiO_2^-] \qquad (9)$$

$$[Cl^-]_T=[Cl^-]+[Bi^{3+}]\sum_{i=1}^{6} i\beta_i[Cl^-]^i \quad (10)$$

Formula (9) was expanded to:

$$[Bi^{3+}]_T=[Bi^{3+}]+\sum_{i=1}^{6}\beta_i[Bi^{3+}][Cl^-]^i+\sum_{j=4}^{4}\alpha_j[Bi^{3+}][OH^-]^j+\frac{[Bi^{3+}]K_2}{[H^+]^2}+\frac{[Bi^{3+}]K_3}{[H^+]^4} \quad (11)$$

where $[Cl^-]_T^0$ and $[Bi^{3+}]_T^0$ were the total concentration of bismuth and chlorine, respectively.

1)equilibrium of BiOCl solution:

From the reaction (3), it was known that 1 mol of bismuth ion and 1 mol of chloride ion were required to form 1 mol of BiOCl; thus we could obtain the following equation:

$$[Bi^{3+}]_T^0-[Bi^{3+}]_T=[Cl^-]_T^0-[Cl^-]_T \quad (12)$$

By substituting equations (10) and (11) into equation (12), we could obtain:

$$[Bi^{3+}](1+\sum_{i=1}^{6}(1-i)\beta_i[Cl^-]^i+\sum_{j=1}^{4}\alpha_j[OH^-]^j+\frac{K_2}{[H^+]^2}+\frac{K_3}{[H^+]^4})=[Bi^{3+}]_T^0-[Cl^-]_T^0+[Cl^-]_T \quad (13)$$

When pH≥2, $[Cl^-]$ was approximately equal to $[Cl^-]_T^0-[Bi^{3+}]_T^0$, which was a constant;

Substituting the reaction formula (3) into the formula (9), we could obtain:

$$[Bi^{3+}]_T=\frac{[H^+]^2}{K_1[Cl^-]}(1+\sum_{i=1}^{6}\beta_i[Cl^-]^i+\sum_{j=1}^{4}\alpha_j[OH^-]^j+\frac{K_2}{[H^+]^2}+\frac{K_3}{[H^+]^4}) \quad (14)$$

2)equilibrium of Bi_2O_3 solution:

Similarly, when *p*H≥2, $[Cl^-]$ was approximately equal to $[Cl^-]_T^0$, which was also a constant;

Substituting the reaction formula (6) into the formula (9), equation (15) can be obtained:

$$[Bi^{3+}]_T=\frac{[H^+]^3}{K_4^{1/2}}(1+\sum_{i=1}^{6}\beta_i[Cl^-]^i+\sum_{j=1}^{4}\alpha_j[OH^-]^j+\frac{K_2}{[H^+]^2}+\frac{K_3}{[H^+]^4}) \quad (15)$$

3)equilibrium of Bi_3O_4Cl solution:

The formation of 1 mol of Bi_3O_4Cl required 3 mol of bismuth ions and 1 mol of chloride ions, shown as follows,

$$[Bi^{3+}]_T^0-\frac{1}{3}[Bi^{3+}]_T=[Cl^-]_T^0-[Cl^-]_T \quad (16)$$

Similarly, when pH≥2, $[Cl^-]$ was approximately equal to$[Cl^-]_T^0-\frac{1}{3}[Bi^{3+}]_T^0$, which was a constant.

Substituting the reaction formula (7) into the formula (9), then:

$$[Bi^{3+}]_T=\frac{[H^+]^2}{(K_5[Cl^-])^{1/3}}(1+\sum_{i=1}^{6}\beta_i[Cl^-]^i+\sum_{j=1}^{4}\alpha_j[OH^-]^j+\frac{K_2}{[H^+]^2}+\frac{K_3}{[H^+]^4}) \quad (17)$$

4)equilibrium of Bi_2O_3 solution:

Similarly, when pH≥2, $[Cl^-]$ was approximately equal to $[Cl^-]_T^0$, which was a constant.

Substituting the reaction formula (8) into the formula (9), then:

$$[Bi^{3+}]_T=\frac{K_{sp}}{[OH^-]^3}(1+\sum_{i=1}^{6}\beta_i[Cl^-]^i+\sum_{j=1}^{4}\alpha_j[OH^-]^j+\frac{K_2}{[H^+]^2}+\frac{K_3}{[H^+]^4}) \quad (18)$$

When the total concentration of bismuth and the total concentration of chlorine were given, the relationship between *p*H and $lg(Bi^{3+})$ was made by the above formulas (14), (15), (17) and (18), as shown in Figure 3. The figure shows the equilibrium line between the solid phase and the liquid phase. The area above the curve was the solid phase stability zone. The area below the curve was the liquid phase stability zone. It can be divided into four solid phase stability zones, namely BiOCl, Bi_2O_3, $Bi(OH)_3$ and Bi_3O_4Cl. In the Bi^{3+}-Cl-H_2O system, when the control $3<pH<5$, stable BiOCl and Bi_3O_4Cl could be formed, so that the Bi^{3+} hydrolysis verification experiment in the chloride salt system was chosen to adjust the *p*H to 4.

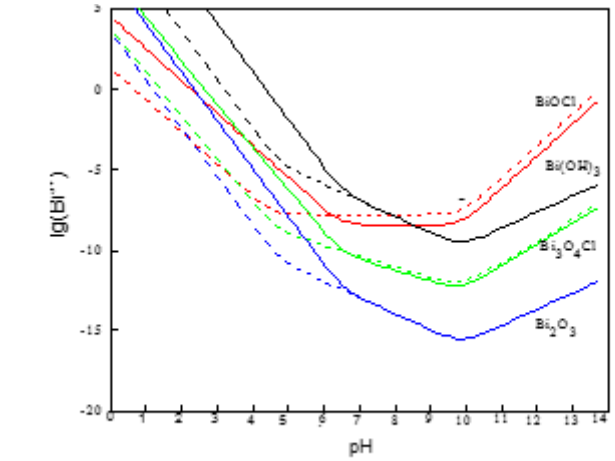

Figure 3. Relationship between *p*H and lg(Bi^{3+}) of hydrazine hydrolysis in chloride system

3.3 Analysis of bismuth hydrolysis mechanism under chlorine salt system by infrared spectroscopy

The filtrates of $BiCl_3$ hydrolytic action, alcoholysis reaction and alcoholysis reaction with ethylene glycol were characterized by infrared spectrum, and blank experiment was performed for comparative analysis to verify the reaction path of $BiCl_3$ in the hydrolysis process and the conversion mechanism of chlorine oxygen [38-39]. The results are shown in Figure 4 to Figure 7, and the characteristic infrared peaks are shown in Table 8.

Table 8. Infrared characteristic peak

Key type	O-H	C-C	Alcohol C-O	-CH_3	-CH_2-
Absorption peak position (cm^{-1})	3350~3200（stretch）~1595（bending）750~650（Out-of-plane bending）	400~900	1260~1000	~2870（symmetry）~2960（Asymmetry）~1380（Symmetric deformation）	~2925（Asymmetry）~2850（symmetry）1480~1440（Scissor）

3.3.1 Infrared spectroscopy analysis of $BiCl_3$ solid hydrolysis in Bi^{3+}-Cl-H_2O system

It can be seen from curves A and B in Figure 4 that, a peak occurred at 3313.21 cm^{-1} assigned to O-H stretching vibration, and a peak occurred at 1643.38 cm^{-1} assigned to bending vibration of O-H molecules. On the one hand, due to the addition of $BiCl_3$ and its hydrolysis, the degree of hydroxyl ionization in water was strengthened, the number of free hydroxyl groups in water was increased, and the concentration of hydroxyl groups was relatively large. On the other hand, due to the ionization of $BiCl_3$ after $BiCl_3$ was added, Bi atom replaced H atom of water ([H-OH]) to form a [Bi-OH] monomer. In the [Bi-OH] monomer, there was a hydrogen bond between the oxygen atom in the OH and another water molecule, which was not easy to be broken; the electronegativity of chlorine was 3.16, the electronegativity of hydrogen in water was 2.1, and free Cl ions were generated in water. It was easy to replace the hydrogen atom in the water hydroxyl group to form [Cl-O-Bi], which was BiOCl, and the Bi atomic nucleus was larger than the H nucleus. It was easy to form $Bi[OH]_3$ with the hydroxyl group generated by water ionization. Since $Bi[OH]_3$ was unstable, it would continue to hydrolyze to form BiOCl or Bi_3O_4Cl. Cl atom was replaced by the H atom in the water hydroxyl group, and therefore, the electron cloud density increased, the force constant k increased, and the induction effect occurred. The group frequency shift to a high wave number, and correspondingly, the infrared spectrum of the water had a red shift. The stronger the electronegativity of the element, the stronger the induction effect, and the more obvious the shift of the position of the absorption peak to the high wave number[40-41]. Comparing curves A and B in Figure 4, the absorption peak at 1643.38 cm^{-1} only shift to the peak by

0.25 cm^{-1}, and the absorption peak at 3313.21 cm^{-1} shift by 9.22 cm^{-1}, which demonstrates that the red shift of the absorption peak at 3313.21 cm^{-1} was not only due to the increase of the hydroxyl group concentration in the solution, but also due to that the chlorine replaced the hydrogen in the water hydroxyl group to induce an effect.

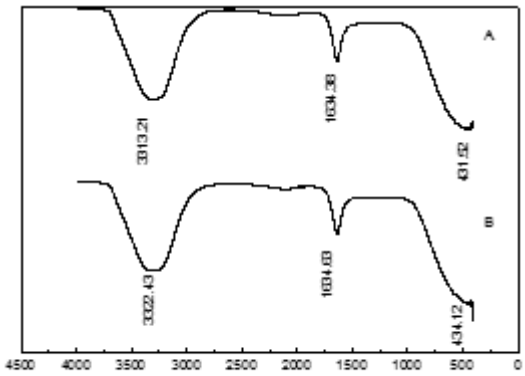

Figure 4. $BiCl_3$ solid hydrolysis

3.3.2 Infrared spectroscopy analysis of $BiCl_3$ solid hydrolysis in Bi^{3+}-Cl-C_2H_5OH system

Comparing curves C and D in Figure 5, the absorption peak at 3316.10 cm^{-1} shift to 3.76 cm^{-1} at the peak region, and the absorption peak at 636.44 cm^{-1} shift to the low peak region by 3.29 cm^{-1}, this was resulted from that the H on the -OH in ethanol was replaced by Cl, which increased the electron cloud density and the force constant k, and induced an effect. Therefore, the group frequency at 3316.10 cm^{-1} shift to a high wave number, and thus, the infrared spectrum of ethanol red-shift. The electronegativity of chlorine was relatively larger than that of hydrogen. The electronegativity of carbon was 2.55, the electronegativity of oxygen was 3.44, the electronegativity of hydrogen was 2.1, and the electronegativity of chlorine was 3.16; so it would replace -OH. After the upper H, a monomer such as [C-O-Cl] was formed. The greater the difference in the electronegativity between the two ends of the bond (the greater the polarity), the stronger the absorption peak, the stronger the polarity, the red shift of the absorption peak. The weaker the polarity, the blue shift of the absorption peak. O-Cl was weaker than -OH, and therefore, the absorption peak at 636.44 cm^{-1} shift to the low peak region, and blue shift occurred, which proves that H atom on -OH was replaced by Cl atom. Since the alcoholysis of $BiCl_3$ was slow in ethanol, ammonia water was added to $BiCl_3$+C_2H_5OH system to promote alcoholysis[42-44]. Comparing curves E and F in Figure 5, the peak at 1642.82 cm^{-1} was excited by stretching vibration of NH-NH_3, wherein the absorption peak at 3358.72 cm^{-1} and the absorption peak at 562.79 cm^{-1} were red at the peak. The shift of 5.98 cm^{-1} and the blue shift of 18.99 cm^{-1} at the low peak further confirmed the substitution of $BiCl_3$ in ethanol.

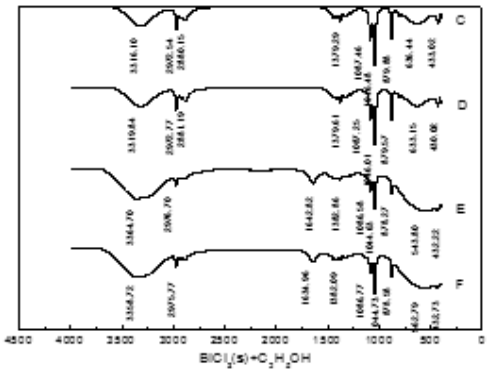

Figure 5. $BiCl_3$ solid ethanol alcoholysis

3.3.3 Infrared spectroscopy analysis of $BiCl_3$ solid hydrolysis in Bi^{3+}-Cl-$(CH_2OH)_2$ system

In order to more clearly understand the mechanism of chlorine and oxygen regulation in the hydrolysis process of $BiCl_3$, it was added to prove whether $BiCl_3$ could undergo alcoholysis in ethylene glycol. Comparing curves G and H in Figure 6, it can be seen that 3297.97 cm^{-1} blue-shift by 4.93 cm^{-1} to the low peak. This was because the electronegativity of chlorine was relatively larger than that of hydrogen, and the electronegativity of carbon was 2.55. The electronegativity was 3.44, the electronegativity of hydrogen was 2.1, and the electronegativity of chlorine was 3.16. Therefore, after hydrogen was replaced by -OH, a monomer such as [C-O-Cl] was formed. The greater the difference in the electronegativity between the two ends of the bond (the greater the polarity), the stronger the absorption peak, the stronger the polarity, the red shift of the absorption peak; the weaker the polarity, the blue shift of the absorption peak. Therefore, the O-Cl was weaker than the -OH polarity, and the absorption peak at 3297.97 cm^{-1} shift to the low peak region, causing a blue shift, which proves that the hydrogen on the -OH was replaced by chlorine. On the other hand, the absorption peak of 881.27 cm^{-1} red-shift by 0.02 cm^{-1} and the absorption peak at 860.18 cm^{-1} blue-shift by 0.4 cm^{-1}, which was due to the unsubstituted -OH in ethylene glycol adjacent. The other -OH hydrogen was replaced by chlorine, resulting in the substitution of -OH; the electron cloud density increased, the force constant k increased, and the induced effect occurred, causing the absorption peak at 881.27 cm^{-1} to shift to a high wave number. The infrared spectrum of the diol slightly red-shift while the other was not replaced, so a blue shift occurred. Since the alcoholysis of $BiCl_3$ in ethylene glycol was extremely slow and almost no alcoholysis occurred, ammonia water was added to $BiCl_3$+$(CH_2OH)_2$ system to promote alcoholysis[45] .Comparing I and J in Figure 6, the peak at 1643.32 cm^{-1} was generated by the stretching vibration of NH-NH_3; comparing curves E and F, the absorption peak at 3284.52 cm^{-1} had a blue shift of 3.47 cm^{-1} , the absorption peak at 882.33 cm^{-1} had a blue shift of 0.4 cm^{-1}, and the absorption peak at 860.99 cm^{-1} had a red shift of 0.49 cm^{-1}, which further confirmed the substitution of $BiCl_3$ in ethylene glycol. The above proof was verified, and an absorption peak was added at 1643.27 cm^{-1}, which was generated by the —NH stretching vibration.

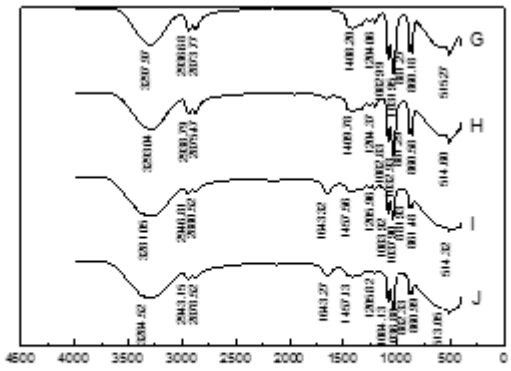

Figure 6. $BiCl_3$ solid glycol alcohol hydrolysis

3.3.4. Hydrolysis mechanism of $BiCl_3$ liquid in Bi^{3+}-HCl system

In order to verify whether the hydrolysis, alcoholysis, and glycolysis of solid $BiCl_3$ were hydrolyzed, a simulated liquid test was performed. The above experiment was carried out by formulating a certain concentration of $BiCl_3$ solution, and the same conditions were applied for infrared analysis. The final results are shown in Figure 7 (1), Figure 7 (2), and Figure 7 (3). The results were consistent with the results of Figure 4, Figure 5, and Figure 6, respectively, because the analysis results were basically the same, no more tautology here.

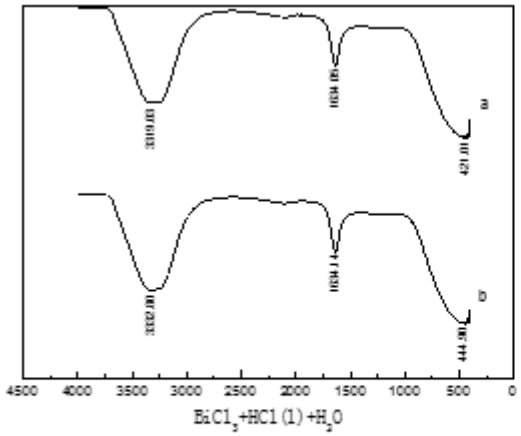

(1) Infrared spectra of $BiCl_3$+HCl(l)+H_2O

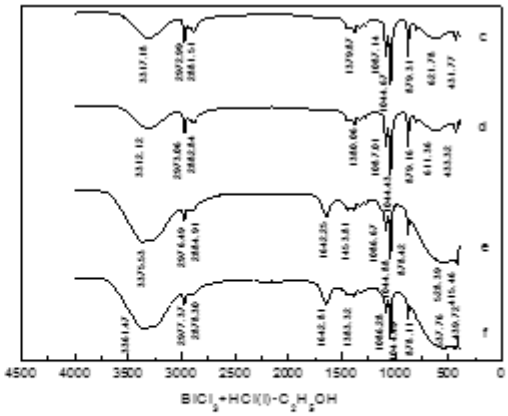

(2) Infrared spectra of $BiCl_3$+HCl(l)+C_2H_5OH

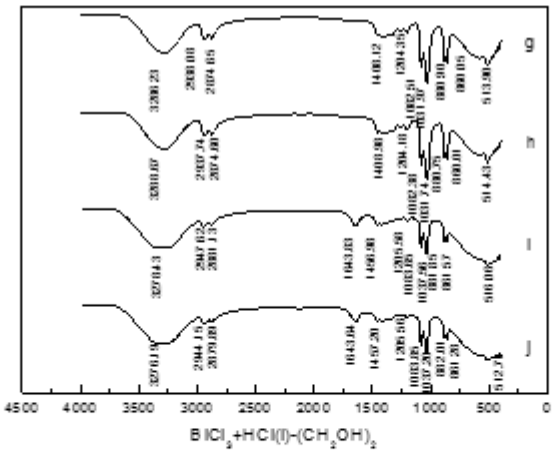

(3) Infrared spectra of $BiCl_3$+HCl(l)+ $(CH_2OH)_2$

a-HCl+H_2O b-$BiCl_3$+HCl+H_2O c-HCl+C_2H_5OH d-$BiCl_3$+HCl+C_2H_5OH

e-$BiCl_3$+HCl+C_2H_5OH+NH_3 · H_2O f-C_2H_5OH+HCl+NH_3 · H_2O g-HCl+$(CH_2OH)_2$

h-$BiCl_3$+HCl+$(CH_2OH)_2$ i-$BiCl_3$+HCl+$(CH_2OH)_2$+NH_3 · H_2O

j-$(CH_2OH)_2$+HCl+NH_3 · H_2O

Figure 7. $BiCl_3$ + HCl (l) liquid hydrolysis, ethanol alcoholysis, glycol alcoholysis

4.Conclusions

The electronic properties of $BiCl_3$, BiOCl and Bi_3O_4Cl cells were calculated by density functional method here. The valence bond properties of the cell structure of $BiCl_3$, BiOCl and Bi_3O_4Cl were analyzed from the respects of unit cell structure, unit cell energy, band structure, total density of states, partial density of states, Mulliken population and overlapping population. The atomic transfer pathway of BiOCl and Bi_3O_4Cl formed during the hydrolysis of $BiCl_3$ was further analyzed by infrared spectroscopy. There were two main ways to prove that $BiCl_3$ was hydrolyzed into oxychloride. One was that the [Bi-Cl] ionic bond between $BiCl_3$ was broken, and the hydroxide replaced the chlorine atom to form $Bi(OH)_2Cl$. $Bi(OH)_2Cl$ was extremely unstable in aqueous solution, and it was easy to continue hydrolysis. It contained two hydroxyl groups that were easy to combine with each other and lose a part of water. The other one was that the hydroxyl groups contained in $Bi(OH)_2Cl$ tended to react with H^+ in aqueous solution and lose a molecule of water. The number of $Bi(OH)_2Cl$ reactions involved determined the degree and complexity of the formation of a series of chlorinated compounds ($Bi_xO_yCl_z$). The ruthenium atom easily formed a [Bi-OH] monomer with a hydroxyl group, and the chlorine atom directly formed a BiOCl instead of a hydrogen atom on the hydroxyl group of the [Bi-OH] monomer.

Infrared spectroscopy shows that under water, ethanol and ethylene glycol systems, water hydroxyl and alcohol hydroxyl groups had red-shift and blue-shift, respectively; the hydroxyl vibration in the high-wave region was caused by the substitution of chlorine atoms for hydrogen atoms, which increased the density of electron clouds, increased the force constant k, and induced effects. The group frequency shift to high wavenumbers, and the infrared spectrum shift red. -OCl was relatively weaker than -OH, so the hydroxyl vibration at the low peak region shift to the low peak region, causing a blue shift, which proved that the hydrogen atom on the -OH was replaced by a chlorine atom. It was consistent with the strength of the covalent bond between the calculated chlorine and oxygen, and the results of the density functional method were further verified using experimental results.

References

1.CHEN YUMENG, TONG XIONG, LV HAOZI. Experimental research on retrieve bismuth from Cu-Bi sulfide ore [J]. Mineral Resources.2018,(2) : 25-27,56.
2.GUO RUI, LIU DAN, GUO ZHI-QIANG, WANG YI-JIE, XIA JIE, WEN SHU-MING. Test on beneficiation of bismuth metal from copper tailings [J]. Mining and Metallurgy.2018,27(3) : 13-17, 27.
3.HA T K , KWON B H , PARK K S , et al. Selective leaching and recovery of bismuth as Bi_2O_3 from copper smelter converter dust[J]. Separation and Purification Technology, 2015, 142:116-122.
4.ZHANG B, LI Q, SHEN W, et al. Recovery of bismuth and antimony metals from pressure-leaching slag[J]. Rare Metals, 2012, 31(1):102-106.
5.BAI MENG, JI HONG-WEI, LI GUANG-MING, XU FENG-PING. Bismuth industrial production process and application [J]. Copper Engineering, 2015(2):8-10.
6.PENG WEN, ZHONG LIPING, LIU HANG, LU JICHANG, LUO YONGMING, GAO XIAOYA. Research progress in selective photocatalytic oxidation of organic pollutants [J]. Technology of Water Treatment.2017,43(4) : 1-5, 10.
7.HE PING, CHEN YONG, FU WEN-FU. Study of Visible-light Driven Preparation of Fe/g-C_3N_4 Composite Catalyst with Simultaneous Hydrogen Evolution [J]. Journal of Molecular Catalysis(China).2016,(3) : 269-275.
8.ZHU, YAHUI,SI, HUAYAN,SUN, XIUGUO, et al.Preparation and characterization of bifunctional $BiOCl_xI_y$ solid solutions with excellent adsorption and photocatalytic abilities for removal of organic dyes[J].Materials science in semiconductor processing,2016,41:193-199.
9.LANG CHEN, JIE HE, YING LIU, PENG CHEN, CHAK-TONG AU, SHUANG-FENG YIN. Recent advances in bismuth-containing photocatalysts with heterojunctions [J]. Chinese Journal of Catalysis.2016,37(6) : 780-791.
10.ZHANG XIAO-JING, ZHAO ZI-YAN, XIONG ZHUO, CHEN MENG-LU, WANG FANG, ZHOU YING. Graphene-bismuth based oxide composite photocatalytic materials [J]. Journal of Functional Materials.2014,(16) : 16001-16008, 16013.
11.JUNXIU WANG, ZHENZONG ZHANG, XI WANG, YI SHEN, YONGFU GUO, PO KEUNG, WONG RENBI BAI. Synthesis of novel p-n heterojunction m-Bi_2O_4/BiOCl nanocomposite with excellent photocatalytic activity through ion-etching method [J]. Chinese Journal of Catalysis.2018,39(11) : 1792-1803, 1911-1913.
12.SCHLESINGER M, PATHAK A, RICHTER S, et al. Salicylate-Functionalized Bismuth Oxido Clusters: Hydrolysis Processes and Microbiological Activity[J]. European Journal of Inorganic Chemistry, 2015, 2014(25):4218-4227.
13.L, MIERSCH T, RÜFFER M, SCHLESINGER H, et al. Hydrolysis studies on bismuth nitrate: synthesis and crystallization of four novel polynuclear basic bismuth nitrates.[J].Inorganic chemistry,2012,51(17):9376-84.
14.LIU HONGQI, GU XIAONA, CHEN FENG, ZHANG JINLONG. Preparation of Nano BiOCl Microsphere and Its Fabrication Machanism[J]. Chinese Journal of Catalysis,2011,32(1):129-134.

15.NARSAIAH A V , REDDY B V S , PREMALATHA K , et al. Bismuth(III)-Catalyzed Hydrolysis of Epoxides and Aziridines: an Efficient Synthesis ofvic-diols and β-Amino Alcohols[J]. Catalysis Letters, 2009, 131(3-4):480-484.
16.ZHANG CHUANFU, DING FENGHUA, ZHAN JING, WANG ZHIJIAN, WU JIANHUI, CAO WENXIN. A Novel Process for Solvent Extraction of Bismuth and Preparation of Bi2O3 From BiCl3 Solution[J]. Hydrometallurgy of China,2015,34(1).
17.XIA JI-YONG, TANG MO-TANG, CHEN CUI, JIN SHENG-MING, CHEN YONG-MING. Preparation of α-Bi_2O_3 from bismuth powders through low-temperature oxidation [J]. Transactions of Nonferrous Metals Society of China.2012,(9)：2289-2294.
18.XIA JI-YONG, TANG MO-TANG, CHEN CUI, CEN YONG-MING, LU JIE-ZHU. Theoretical and Technical Studies on Bismuth Trioxide Preparation by Low-temperature Oxidation Method[J]. Mining and Metallurgical Engineering.2012,(1)：102-106.
19.HE JING, TANG MO TANG, LU JUN LE, TANG WEN LI. Preparing Bi_2O_3 from Bismuth Powder in the Chloride System [J]. Mining and Metallurgical Engineering.2002,(1)：76-79.
20.WU WEN-WEI, LAI SHUI-BIN, SU PENG, LIAO SEN,SUN Preparation of nanometer bismuth oxide from bismuth oxychloride via liquid-state transformational method and thermal properties of its precursor [J]. Applied Chemical Industry,2006(5):335-338.
21.ZHENG GUOQU, CAO HUAZHEN, TANG MOTANG. Study on dechlorination in process of preparing high purity Bi_2O_3 fron BiOC [J]. Nonferrous Metals.2001,53(2)：52-54.
22.ZHENG GUOQU, TANG MO TANG. Phases of residue in distillation of $BiCl_3$-HCl-H_2O system[J]. The Chinese journal of nonferrous metals, 2000, 10(2):250-252.
23.CLARK S J , SEGALLII M D , PICKARDII C J, et al. First principles methods using CASTEP[J]. Zeitschrift für Kristallographie, 2005, 220(5-6).
24.MILMAN V, REFSON K , CLARK S J , et al. Electron and vibrational spectroscopies using DFT, plane waves and pseudopotentials: CASTEP implementation[J]. Journal of Molecular Structure Theochem, 2010, 954(1):22-35.
25.NI Z , GUO X , LIU X , et al. Understanding the magnetic structural transition in all-d-metal Heusler alloy $Mn_2Ni_{1.25}Co_{0.25}Ti_{0.5}$[J]. Journal of Alloys and Compounds, 2019, 775:427-434.
26.FRANCISCO C , FERNÁNDEZ ANA MARÍA, TIMÓN VICENTE, et al. Becquerelite mineral phase: crystal structure and thermodynamic and mechanical stability by using periodic DFT[J]. RSC Advances, 2018, 8(43):24599-24616.
27.DENG Y , EAMES C , NGUYEN L H B, et al. Crystal structures, local atomic environments and ion diffusion mechanisms of scandium-substituted nasicon solid electrolytes[J]. Chemistry of Materials, 2018:acs.chemmater.7b05237.
28.XIAO X , XING C , HE G, et al. Solvothermal synthesis of novel hierarchical $Bi_4O_5I_2$ nanoflakes with highly visible light photocatalytic performance for the degradation of 4-tert-butylphenol[J]. Applied Catalysis B: Environmental, 2014, 148-149:154-163.
29.YUAN S, SUN Z, REN W, et al. First principles study of the magnetic properties and charge transfer of Ni-doped $BiFeO_3$[J]. Journal of Magnetism & Magnetic Materials, 2017, 449:S0304885317307461.
30.ZHANG S Y, HU C L, LI P X, et al. Syntheses, crystal structures and properties of new lead(II) or bismuth(III) selenites and tellurite[J]. Dalton Transactions, 2012, 41(31):9532-9542.
31.JIANG H Y , LI P , LIU G, et al. Synthesis and photocatalytic properties of metastable β-Bi_2O_3 stabilized by surface-coordination effects[J]. Journal of Materials Chemistry A, 2015, 3.
32.WU C , LU P , YU Z , et al. Structural and Electronic Properties of Neutral Clusters $Al_{12}X$ (X = P, As, Sb, and Bi) and Their Cations[J]. Journal of Computational and Theoretical Nanoscience, 2013, 10(5):1055-1060.
33.ZHANG XUYUN, ZHENG BINGJIE, GUO BIN, LU HAIJUN, WU ZHUANG. First Principles Study on Electronic Structure and Corrosion Resistance of Fe-N-Cr [J]. Materials Review, 2016,

30(18):155-158.
34. WANG MING-JUN, LI CHUN-FU, WEN PING, ZHANG FENG-CHUN, WANG YAO, LIU EN-ZUO. The bond characters and phase stability effects of Cr Mo and Ni in bulk γ-Fe(C) [J]. Acta Physica Sinica, 2016, 65(3):246-255.
35.ZHANG, PENG;ZHAO, QICHEN;LIU, JINGJUN;et al.Research on inhibitors and hindered groups in ultra-deep hydrodesulfurization based on density functional theory[J].Catalysis Today.2018 : 170-178.
36.XUE JINXIANG, ZHANG XINGGUANG, LIU YANPING, et al. The alloying effect of Ti, C, N in a-Fe matrix and its influence on the bonding properties [J].
37.WEN PING, LI CHUNFU, ZHAO YI, et al. First-principles study on the position, bonding properties and alloying effect of Cr, Mo, Ni in bulkα-Fe (C)% Cr, Mo, Ni account for α-Fe (C) [J]. Acta Phys. Sin, 2014, 000 (019): 1-8.
38.YANG JINMEI, ZHANG HAIMING, WANG XU, WANG CAIXIA, QIN FEIFEI. The relationships and differences between the infrared spextrometry and raman spectrometry [J]. Physics and Engineering, 2014, 24(4):26-29.
39.WANG JING-ZUN, WANG TING. How to Interpret Infrared(IR) Spectra [J]. University Chemistry,2016,31(6):90-97. DOI:10.3866/PKU.DXHX201504001.
40.YUAN BO, DOU XIAO MING. Near Infrared Spectral Studies of Hydrogen Bond in Water-Methanol Mixtures [J]. Spectroscopy and Spectral Analysis,2004,24(11):1319-1322. DOI:10.3321/j.issn:1000-0593.2004.11.011.
41.ROCHA, BRUNO G. M.,POMBEIRO, ARMANDO J. L.,KUZNETSOV, MAXIM L., et al.Simple soluble Bi(III) salts as efficient catalysts for the oxidation of alkanes with H_2O_2[J]. Catalysis science & technology, 2015,5(4):2174-2187.
42.XIE YI, YI JUAN, ZHANG SHU, CHENG HUA-SHENG, SU PING, SHI YONG-GANG. Study on ternary mixtures of water, acetic acid and ethanol by near infrared spectroscopy[J].Chinese Journal of Spectroscopy Laboratory,2003,20(5):643-646. DOI:10.3969/j.issn.1004-8138.2003.05.002.
43. WU XIAOJING, SONG LULU, PAN YAN. Study on Solvation of LiCl, $MgCl_2$ and $CaCl_2$ in Ethanol [J]. Bulletin of Chemistry (printed edition), 2010, 73 (3): 246-251.
44. WU XIAOJING, CHEN XINGLI. Study on the Infrared Spectra of Ethanol under Action of Mg^{2+} [J]. Bulletin of Chemistry (Printed Edition), 2009, 72 (6): 561-564.
45.ZHU CHUAN-GAO, WANG FENG-WU, XU MAI, FANG WEN-YAN. Synthesis of Metal Alkoxide Complex and Nano-$NiFe_2O_4$ in $HOCH_2$-CH_2OH Solution [J].Chinese Journal of Inorganic Chemistry,2009,25 (7):1177-1181. DOI:10.3321/j.issn:1001-4861.2009.07.007.

Manuscript received: 13.02.2020